

# A Turbine Test Facility for Aerodynamic Testing

Lars O Lindqvist<sup>1</sup>      Jonas N Hylén  
ALSTOM Power Sweden AB  
Department of Research & Development  
SE-612 82 Finspong  
Sweden

## ABSTRACT

A turbine test facility at the department of Heat and Power at Kungliga Tekniska Högskolan (Royal Institute of Technology), Stockholm has been running for several years. The facility has during the last year been upgraded, and has been equipped with a new measurement system. The aim of this report is to present the facility and to present some result from different measurements of a meridional profiled test turbine stage.

The test stand was equipped with a single turbine stage during the tests reported in this paper. However, one to three stages can be investigated.

Two different kinds of investigations are presented. The first is the performance measurement, where the stage efficiency is investigated. The second is the cavity flow behaviour, with respect to spanwise temperature distribution. The cavity flow enters the main gas flow between the stator and the rotor at the hub section. The results, of the performance measurement, shows that the test turbine facility works perfectly and that the results is as what can be expected.

The test turbine has been modified in such manner that leakage air from the stator rotor cavity penetrates the main airflow downstream the stator in a slot at the hub section. This airflow has been seeded with a known amount of a trace gas (CO) in order to represent a temperature distribution.

## NOMENCLATURE

A	Area,	m <sup>2</sup>
C	Chord of rotor, velocity	m, m/s
D	Diameter	m
h	Enthalpy	kJ/kg
H	Rotor height	m
L	Specific work	J/kg
$\dot{m}$	Mass flow	kg/s
M	Torque	Nm
N	Speed of revolution	rpm
P	Power	w
p	Pressure	Pa

$\rho$	Density	kg/m <sup>3</sup>
T	Temperature	K
R	Gas constant	J/kg,K
$\kappa$	Ratio of specific heat	-
n	Speed of revolution	RPM
$\nu$	Viscosity	kg/s m
$\eta$	Efficiency	-

## Subscript

21	At measurement plane 21
50	At measurement plane 50
s	Isentropic condition

## INTRODUCTION

The design of new axial turbomachinery demands detailed knowledge of the flow through the stator and rotor cascades. Some of the design tools used for that are the one dimensional mid section calculation, the two dimensional throughflow calculation, the two dimensional blade to blade calculation and finally three-dimensional inviscid and/or viscid calculations.

Despite of all effort spent on numerical calculations the exact details of the real flow conditions are very hard to predict. The need for an experimental facility is thus of great importance. The test turbine stand described in this paper is mainly intended for performance measurements and for investigations of the main flow. But with small amount of work other applications such as stator rotor rim sealing, leakage airflow etc. can be investigated.

The test turbine is situated at the Royal Institute of Technology (KTH) in Stockholm, at the department of Heat and Power Technology, and is a co-operation between ALSTOM Power Sweden AB, (former ABB Stal AB) and KTH.

## THE TEST TURBINE FACILITY

The test turbine is an air driven low-temperature low-pressure test facility test turbine facility can be seen. The inlet housing is at position 10, and the exit stack at section 60.. In Table 1, Fig. 1 and Fig. 2 the main data and main layout of the

<sup>1</sup> Phd Student at the Royal Institute of Technology, Stockholm

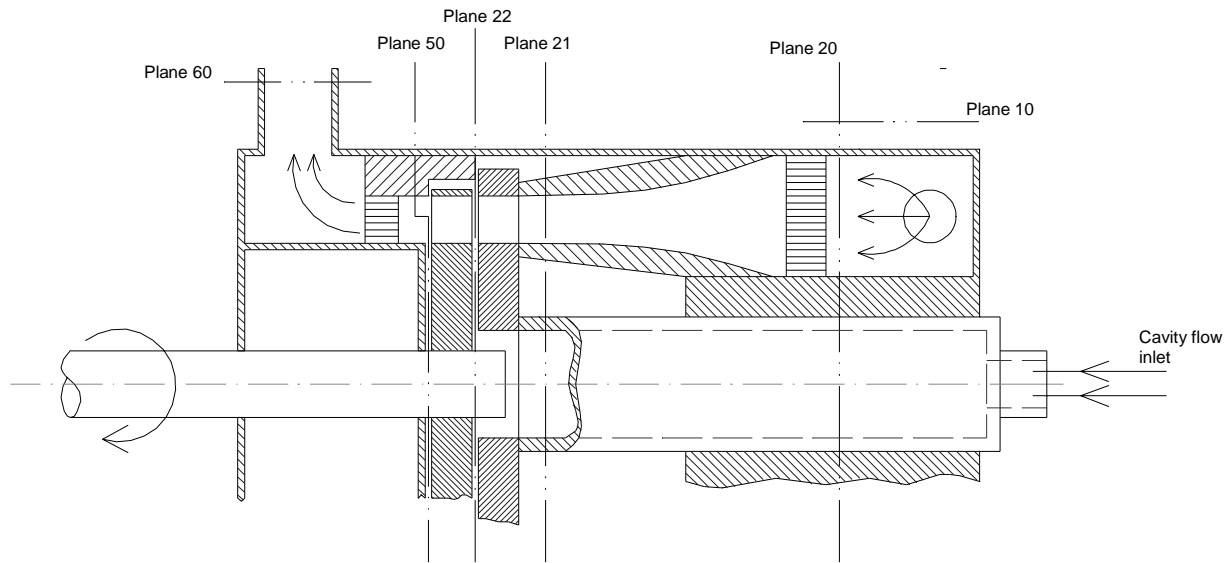


**Fig. 1** Main layout

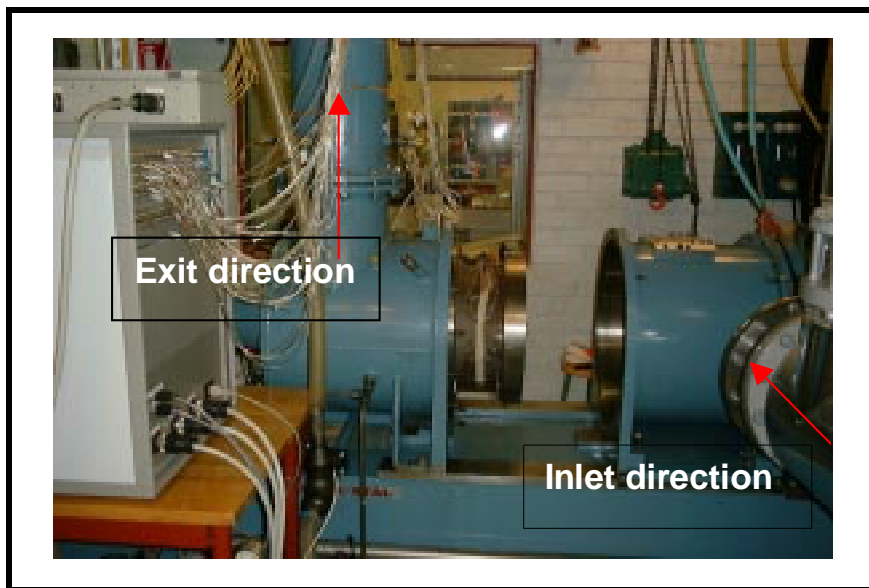


**Fig. 2** The test turbine with the inlet and middle casing open

### **Mechanical design**

The test turbine housing consists of three main parts, the inlet casing, the middle casing and the exit casing. Between the inlet casing and the entrance of the middle casing and also between the discharge section of the middle casing and the entrance of the exit casing bolt coupling in flanges at the periphery of the housings are used for assembly. Consequently, when the turbine shall be opened it is done by removing these bolt couplings, and move the inlet casing or both the inlet casing and the middle casing in the upstream direction, see Fig. 2. The outlet casing is fixed at the foundation. In

order to facilitate the moving of the inlet and middle casing a specially designed air system exists. The air from this system is guided to channels between the foundation and the support of the casing, allowing the casing to be carried with an air cushioning. This procedure makes it very easy to open the turbine when modification or inspection of probes etc. is necessary.

The stators are assembled on an axis, which goes through the inlet casing, and out in the upstream side of the turbine facility. When pitchwise traversing data is needed this axis is rotated. The axis is tubular and allows air to pass through when investigation of e.g.

stator-rotor rim sealing are performed. This design also has the opportunity to evacuate the disc cavity air, by applying a negative pressure.

The rotor blades are mounted on the rotor axis that extends out in the downstream side of the test turbine facility. The shaft torque is measured using a torque meter, which also gives the shaft speed of revolution. The power of the shaft is dissipated into heat in a water brake. The shaft is mounted in a ball bearing. The ball bearing is in turn mounted in a hydrostatic slide bearing. This gives the opportunity to measure the friction torque with a strain gauge. Adding the torque of the shaft and the torque of the bearing friction then give the total torque from which the turbine output power can be determined, see below. The internal calibration of the bearing friction has shown to give accuracy better than  $\pm 0.03\%$ .

At the top of the middle casing holes with probe connections are placed at three locations, upstream the stator, between the stator and the rotor and downstream the rotor, section 21, 22 and 50 in Fig. 1. At this sections stepping motors with probes mounted can be placed when traversed data are needed. These traversing are done in the radial direction. In order to traverse in tangential direction the whole stator cascade is traversed by rotating the shaft that the stators are mounted on, as mentioned above. By doing both these traversings in sequence the whole flow field can be obtained at the three above mentioned planes.

### The air system

The air to the turbine is supplied from a screw compressor. The compressor delivers air at a maximum total pressure of 4 bar absolute and a massflow rate of max 4.7 kg/s. Downstream of the compressor the air temperature is controlled by a cooler, to a predetermined temperature between 30°C and 180°C. A condense separator is placed downstream of the cooler in order to minimise the water fraction in the air. Upstream the radial inlet of the turbine stand, the mass flow is measured using an ISO 5167 –standard orifice flange, see Fig. 3. The airflow is regulated by valves of butterfly type, controlled from the operating room. Since the flow enters in the radial direction a honeycomb plate is placed downstream the inlet of the test stand, followed by two perforated plates. This is in order to support a homogenous axial flow to the test section. Downstream the test section, a fan in the outlet stack compensates for the friction losses in the outlet piping. Data of the air system can be seen in Table 1.

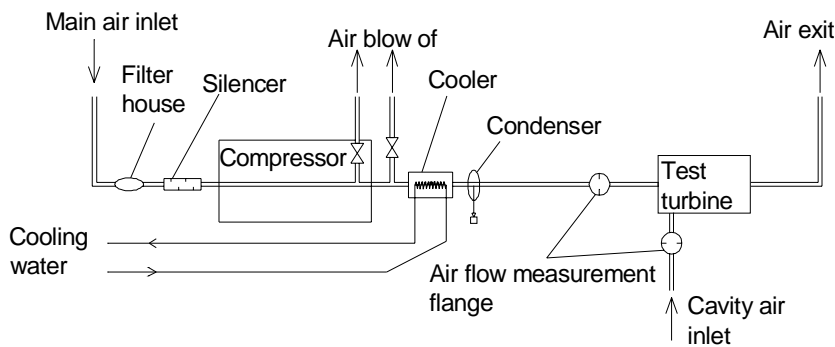


Fig. 3 Main flow scheme

### The investigated geometry

The investigated geometry is a stage intended for a high-pressure steam turbine. The stator is meridional profiled in order to decrease the radial pressure gradient that a conventional designed stage suffers from, see Fig. 4.

The basic idea of the meridional profiling is to eliminate the flow turning due to the cylindrical turbine environment and thus make the flow only turn in a plane. This is done by profiling the endwalls, in a way which make a fluid particle to move in a plane instead of a cylindrical trajectory, and leaning of the stator blades. The meridional profiling, in this investigation, is only applied at the stator casing endwall. The reason for that is to avoid manufacturing problem at the hub section. However to realise the meridional profiling it is necessary to “move” the hub endwall contouring to the casing line, this procedure makes the casing endwall profiling more pronounced. A fluid particle at an imaginary spanwise median streamline would then “feel” a contraction at both the casing and the hub.

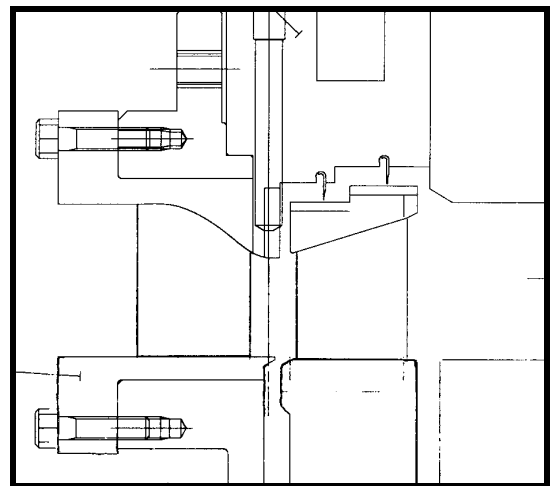


Fig. 4 The test object

Another advantage of the meridional profiling is the enlarged stator entry, which keeps the fluid velocity low until about half a chord, where the flow is rapidly accelerated. Since most flow turning is done in the front part of the stator, the boundary layer movement towards the suction side will be reduced. Also the passage vortices being driven by the boundary layer movement is decreased.

**Table 1**

<b>Air Supply system</b>	
Compressor type	Screw compressor
Max. working pressure	4 bar
Air, massflow	4.7 kg/s
Power input to the compressor	968 kW
Air outlet temperature, at full power	180 °C
Main air pipe inner diameter	300 mm
<b>Turbine Unit</b>	
Number of stators	42
Number of rotors	72
Stator inlet hub/tip ratio	0.84
Rotor inlet hub/tip ratio	0.88
Stator solidity	1.07
Rotor solidity	0.64
Stator inlet aspect ratio	1.33
Rotor inlet aspect ratio	0.96
<b>Flow parameters at design point</b>	
Stator / Rotor exit Mach number	0.48 / 0.11
Pressure ratio, $\pi$	1.23
Stageloaading, $v$	0.55
Flow coefficient	0.31
Degree of reaction	0.14

## DESCRIPTION OF THE MEASUREMENT PLANES

A cross sectional view of the turbine showing the measurement planes was presented in Fig. 1. A short summary of all measurement planes is presented below.

### Plane 20

At the inlet casing, plane 20, the total temperature is measured with four stationary probes. Each probe has two thermocouples mounted at two different radiuses. The total temperature is then considered to be the same at the turbine inlet, plane 21.

### Plane 21

Upstream the stator, at plane 21, the mid span stagnation pressure is measured, with stationary probes, at four tangential positions. Also the static wall pressure, at the hub and tip, are measured at four tangential positions.

### Plane 22

Between the stator and the rotor at plane 22, the total pressure and the flow angle are measured by a traversable four-hole probe. Also the temperature and velocity can be measured by replacing the pressure probe with a thermocouple or a hotwire probe respectively.

When using the hotwire also the turbulence level can be determined. The static wall pressure are measured at four tangential position at both the hub and tip endwalls. Within the cavity, holes for measuring the static wall pressure are seated at the stator disc. These holes can also be used for sampling of concentration measurement during trace gas measurement.

### Plane 50

The total pressure and the absolute flow angle are measured with a traversable probe downstream the rotor in similar manner as in plane 22. The static wall pressure is measured at four tangential positions at the hub and casing lines. Further more the total pressure (at midspan) and the total temperature (at four radial positions) are measured with permanently mounted probes at three tangential positions.

### Plane 60

At the exit housing the total temperature are measured using four stationary mounted temperature probes. Each probe has two thermocouples at two different radiuses.

### Massflow

The massflow of the main flow is measured upstream the turbine with an ISO-standard orifice plate. The same measurement method is used for the disc cavity flow that is supplied to the turbine through the tubular shaft, and enters the main gas path at the hub section between the stator and rotor row.

### The brake torque

The power of the turbine is dissipated in a water brake. Between the turbine and the water brake a torque meter is placed, in order to measure the braking-torque. The signal from the torquemeter is send to a readout unit which displays the shaft power, speed of revolution and the braking torque. Furthermore a digital signal is send to the measurement computer for data saving and data analysis.

### Bearing friction

The bearing friction is measured in order to determine the torque of the bearing friction. It is measured with a strain gauge. The strain gauge measures the tangential force that is transferred from the bearing house, and thus can not be included in the breaking torque.

## THE MEASUREMENT SYSTEM

A new measurement system was installed prior to this investigation. The new system includes a pressure system, and a system for analog data acquisition and a cold junction unit for the thermocouples.

### The cold junction unit

The cold junction unit, CJU, consists of an aluminium plate with three resistant temperature probes for determination of the CJU temperature. The design of the cold junction unit can be seen in Fig. 5. Furthermore the cold junction unit serves as a switchbox for all other electrical signals, e.g. the signals from the bearing friction torque.

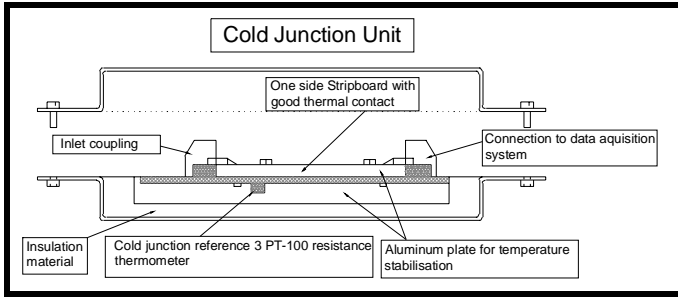


**Fig. 5** The cold junction unit

### The pressure system

The pressure system that is used contains of five separate units connected to each other in a network. The pressure system is manufactured by Pressure Systems Inc. (PSI). Each unit is equipped with 16 individually ranged, true differential, pressure transducer, which gives a total amount of 80 channels, selected data can be seen in Table 2. The accuracy of the pressure system is  $\pm 0.1\%$  of full scale (FS) following single point span calibration. Accuracy of  $\pm 0.15\%$  is maintained for six months after calibration through use of the built in rezero capability. The pressure system is reset to zero before each day of measurement. Zero drift has been checked during one measurement, see Fig. 6 and Fig. 7. These two figures shows pressure for each used pressure transducer before a test started, see Fig. 6, and after the test was finished, see Fig. 7. From Fig. 6 and Fig. 7 it is evident that the zero drift has only minor effect on the accuracy of the pressure measurements. The maximum drift corresponds to an error of 0.037% of full scale (17.5kPa). The time elapsed between the start and stop of the test was approximately 5 hours, which is a normal time of running during a test day.

**Table 2**

PARAMETER	VALUE	UNITS	COMMENTS
Measurement resolution	$\pm 0.003$	% FS	
Static accuracy			
• After rezero	• $\pm 0.15$ • $\pm 0.08$	% FS % FS	Range < 20kPa Range > 20kPa
• After span calibration	• $\pm 0.10$ • $\pm 0.05$	% FS % FS	Range < 20kPa Range > 20kPa
Total thermal error	$\pm 0.001$	$\pm 0.001\%$ FS/°C	
Calibrated temperature range	0 to 50	°C	
Operating temperature range	-20 to 60	°C	
Size	24 x 9 x 10	Cm	L x W x H

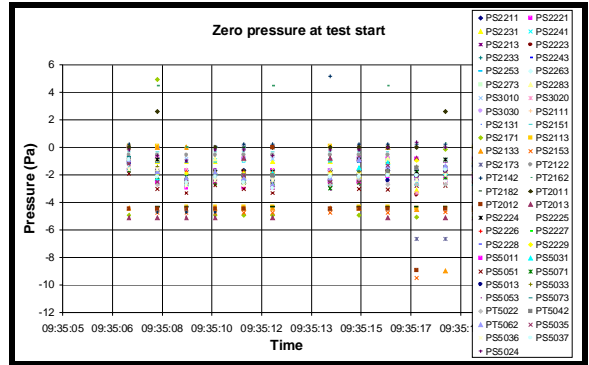


**Fig. 6** Zero pressure at test start

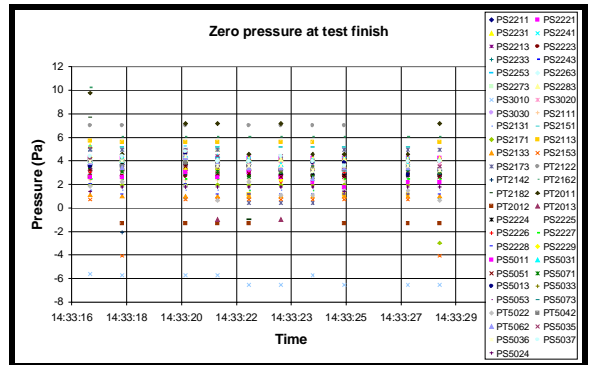


**Fig. 7** Zero pressure after test finish

### The analog data logger system

The system for data acquisition from the thermocouples, torque meter, friction torque, atmospheric pressure and humidity are two Datascan 7220 and one Datascan 7221. The Datascan 7220 unit provides directly 16 analog inputs, but can be connected to a network for extended channels, that is the case for the system used in this investigation. The Datascan 7221 provides 8 analogue inputs including channel excitation, this unit is also integrated in the above-mentioned network. Thus the total amount of channels is 40. The measurement processor of the Datascan units performs the data acquisition and control of the system. A measurement is carried out by an A/D converter. The A/D converter can be programmed to provide either 14 or 16 bits of resolution, for this investigation the resolution was set to 16 bit, that is 1/65536.

### The measurement system installation

The new measurement equipment is installed in a casing. The casing consists of two stories. At the upper storey the five pressure units are installed, and at the lower the three Datascan units, see Fig. 8. On the top of the casing, the cold junction unit (CJU) is placed as a separate unit. The connection between the CJU and the Datascan units in the casing is done via three multi cables connections.



**Fig. 8** The measurement system installed in the casing

The communication between the measurement system and the computer is done by two serial cables, one for the PSI units and one for the Datascan units, between the casing and the computer.

## SETUP /EVALUATION OF PERFORMANCE MEASUREMENT

### Evaluation of the performance

One of the most important figures of merit in turbine testing is the stage efficiency. Within the literature there exists a tremendous amount of different efficiencies defined for turbine application. This section describes the definitions used in this paper.

There are in principle two methods available to determine the stage efficiency based on measurements:

- **Thermodynamically:** By measuring pressure and temperature before and after the turbine stage.
- **Mechanically:** By measuring the massflow, turbine shaft output, pressure before and after the turbine, and the temperature before the turbine.

In this investigation, only the mechanically measured efficiency is used. The definition is described by eq. 1

$$\eta_s^m = \frac{\Delta h_m}{\Delta h_s} \quad (1)$$

The real enthalpy drop,  $\Delta h_m$ , of the stage is measured as:

$$\Delta h_m = L + \frac{C_{50}^2 - C_{21}^2}{2} \quad (2)$$

where:

$$L = \frac{P}{\dot{m}_{tot}} \quad (3)$$

and:

$$P = \frac{M_{tot} \cdot n \cdot \pi}{30} \quad (4)$$

The isentropic enthalpy drop of the stage is measured as:

$$\Delta h_s = cp \cdot T_{21}'' \cdot \left[ 1 - \left( \frac{P_{50}''}{P_{21}''} \right)^{\left( \frac{\kappa-1}{\kappa} \right)} \right] \quad (5)$$

### SETUP FOR CONCENTRATION MEASUREMENT

When using the test turbine for concentration measurements, many different configurations and parameters can be varied. One investigation was performed in order to check what influence the cavity flow (the flow that enters the main flow between the stator and the rotor from the disc cavity) has on the main flow with respect to the radial temperature distribution Lindqvist et al., (2000).

Since the test turbine is a low-pressure low temperature facility, and works typically in atmospheric conditions. The exit temperature of the rotor is in the range of 10 to 20 degree Celsius. By supplying the hub cavity flow with a temperature ratio,  $T_{IT}/T_{cavity}$ , corresponding to a real gasturbine, which normally have  $T_{IT}/T_{cavity} = 2$  in the first stage, results in a temperature of the hub cavity flow of about 150K. During this project such temperature was not realistic to use. Therefore, a trace gas technique was used. The principle of the trace gas technique is rather straight forward and has been used earlier for similar problems Abe et al (1979), Joslyn and Dring (1988), Lewis (1993).

Abe et al. (1979) used the analogy of eq. 6 between the temperature and the concentration rate.

$$\frac{T_m - T_c}{T_{NC} - T_c} = \frac{K_m - K_c}{K_{NC} - K_c} \quad (6)$$

According to that analogy, the following measurement procedure was used in order to experimentally verify numerical result:

1. The temperature,  $T_{NC}$ , is measured at the axial position that shall be investigated. The probe is traversed in several radial and tangential positions without any hub cavity flow present. A pitchwise averaging was performed, leaving only a spanwise distribution. This is the reference case.
2. The test turbine was supplied with air through the cavity and in to the main gas path. The supplied air was seeded with a trace gas, in this investigation CO, and the concentration rate,  $K_c$ , of the air/CO mixture upstream the inlet of the test turbine cavity was measured.
3. The concentration rate,  $K_m$ , was measured at the same positions as  $T_{NC}$ . And also averaged in the same way.
4. The analogy of eq. 6 is used with  $T_c$  determined from the  $T_{IT}/T_{cavity}$  ratio, with  $K_{NC}$  always zero, and the equation was solved for  $T_m$ .  $K_{NC}$  is always since for a non cooled case, i.e. without any hub cavity flow, the concentration rate is zero.

The concentration measurements were taken downstream the rotor rotor by using a Pitot tube. The probe had an outer diameter of 1.6mm. The static pressure before the turbine was measured at plane 20, and the static pressure after the turbine was measured at plane 50. Both as static wall pressures at the endwall. The probe was radial traversed and the whole stator cascade where traversed

pitchwise in order to measure one flow channel. The measurement was performed for different velocity ratios, cavity mass flows and turbine pressure ratios to verify numerically results, Lindqvist et al (2000).

The instrument for measuring the CO concentration is a Rosemount, Binos 100 CO/CO<sub>2</sub> sampler. The signal from the concentration instrument is collected by one of the Datascan channels. The gas analysis is performed by extracting gas from the flow path that is under investigation. This was done by locating the Pitot tube in the main gas channel downstream the rotor, as described above.

The measurement principle of the used gas analyser is by infrared absorption method. That means that an infrared light beam is directed towards a transparent pipe where the gas, which shall be analysed, flow through. The gas acts as a filter and weakens the intensity of the light beam. At the other side of the transparent pipe, a receiver is located. The receiver collects and registers the intensity of the light. Every value is logged once per second. During a measurement the data is saved after 30 second, and the final value of the concentration rate is acquired. The instrument was calibrated before each test run. Several test runs were performed in order to check the repeatability. These tests showed that the maximum relative error between two repeated measurements of the same operating point was less than 5% of the measured value.

## RESULT OF MEASUREMENT

### Performance measurement

One way of presenting the turbine characteristic that is often used involves the rotor velocity-isentropic velocity ratio  $v = U/C_{is}$ , further called velocity ratio, Horlock, (1966). Here  $C_{is}$  is the velocity that would be achieved in an isentropic expansion through the total pressure ratio of the turbine at the entry stagnation temperature. The efficiency can then be plotted as a function of different velocity ratios, and the performance of the turbine can be evaluated from that plot. The measured efficiency was derived from the measurements as described above for the mechanically derived efficiency. Figure 9 shows the measured results for different velocity ratios.

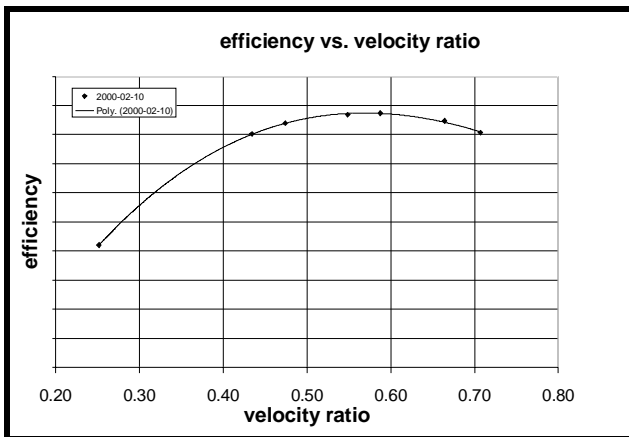


Fig. 9 Measured performance

In Fig. 9 a typical result from a performance measurement is shown. The efficiency is plotted as a function of the velocity ratio. The design point is at velocity ratio 0.55. A decrease in velocity ratio from that operating point will result in a drop of efficiency, which is seen in the plot. The same is valid when the velocity ratio is increased from the optimum point. The major reason for that is that the rotor has to operate with off-design flow angles, but also the pressure gradient within the rotor cascade is changed, that also changes the losses.

### Hub cavity flow measurements

In Fig. 10 measurement of a temperature profile is shown from a measurement when the influence of the cavity flow was studied. The measured normalised temperature distribution that is used is derived as explained in the previous section. Figure 10 shows the experimental results of the dependence of the injected cavity mass flow at 45% chord downstream the rotor trailing edge. The temperature deficit is affected by the amount of the injected cavity flow. The main result of changing the cavity mass flow is a change in the absolute value of the temperature deficit.

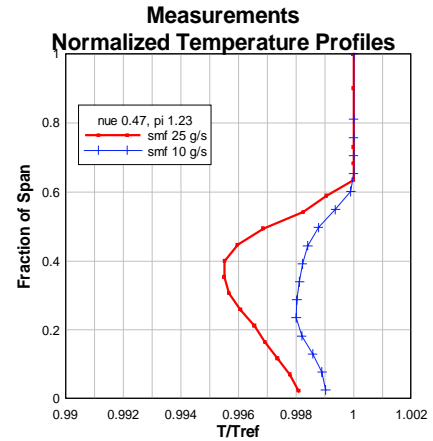
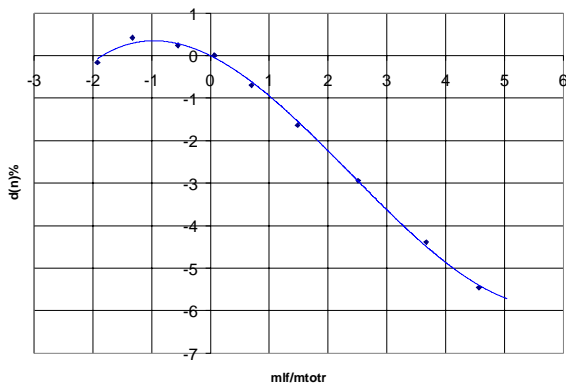


Fig. 10 Rotor exit normalized temperature profile at  $x/C=145\%$

By introducing cavity flow into the main gas path does not only change the temperature redistribution, but what's more important is the influence of the performance of the stage. Figure 11 shows the influence of different cavity flows on the measured performance of the stage. The cavity flow was gradually varied from about 10% of the main flow to a negative value (i.e. suction from the main flow) of 2%. Figure 11 shows that at a negative cavity flow of about 1.5% results in a gain of efficiency of about 0.5%.



**Fig. 11** Cavity flow effect on the performance

## FUTURE WORK

A newly designed two-stage configuration is under manufacturing. Similar tests as reported within this paper are planned to be performed, however the mechanical concept of the stator traverse has to be redesigned.

The approach for that is to have a coupling between the two stator rows allowing each stator row to be rotated individually, or by connecting them and rotate them together. This design allows to investigate the influence of the upstream wake produced by stator row 1 on stator row 2 in order to optimise the pitchwise position between the two stator rows.

Furthermore the stator and rotor profiles are redesigned. Still the stator meridional profiling concept is used both for stage one and stage two but the design point is moved from  $v = 0.55$  to  $v = 0.47$ . Thus this stage operates at a higher stage loading. Also the leading edge of the rotor is changed to a more blunt geometry allowing the incidence angle to be higher.

To make investigation of the cavity flow possible for the second stage a special designed manifold is introduced at the rotor disc.

## REFERENCES

- Abe, T., Kikuchi, J., Takeuchi, H., 1979, "An Investigation of turbine Disk cooling (Experimental investigation and Observation of Hot Gas flow into a Wheel Space)", 13<sup>th</sup> International Congress on Combustion Engines, CIMAC, Vienna
- Joslyn, D., Dring, R.; "A Trace Gas Technique to Study Mixing in a Turbine Stage", *ASME Journal of Turbomachinery*, Vol. 110 pp 38 –43, 1988.
- Horlock, J. H., "Axial Flow Turbines", Butterworth & Co. (Publisher) Ltd, 1966.
- Lewis, K. L., "The Aerodynamics of Shrouded Multi Stage Turbines", Cambridge University, Thesis number DO63469, 1993.
- L. Lindqvist, J. Wickholm, T. Fransson, T. Torisson, 2000, "Investigation of The Spanwise Transport in a Test Turbine Facility", ASME 2000-GT-0489.
- Södergård, B., Henriksson, K., Kjellström, B., Söderberg, O., 1989, "Turbine Testing Facility", TRITA-KRV-1989-03, ISSN 1100-799C.